Radioactive waste as an anthropogenic heat source: shallow and deep geothermal applications

Hannah R. Doran[1,3], Theo Renaud[2], Christopher S. Brown[1], Isa Kolo[1], Gioia Falcone[1] and David C.W. Sanderson[3]

[1] James Watt School of Engineering, University of Glasgow, Glasgow, UK

[2] Department of Engineering Science, University of Auckland, Auckland, New Zealand

[3] Scottish Universities Environmental Research Centre, East Kilbride, UK

h.doran.1@research.gla.ac.uk

Keywords: closed-loop geothermal system (CLGS), U-tube, geological disposal facility (GDF).

ABSTRACT

Unconventional methods to extract heat from the subsurface can play a key role towards achieving net zero greenhouse gas emissions by 2050. A combined numerical/semi-analytical thermal analysis of notional 'Eavor-like' U-tube installations in three different geological disposal facility (GDF) settings is presented. The three geological environments are representative of evaporite (EV), higher strength rock (HSR) and lower strength sedimentary rock (LSSR), at depths of 1, 3 and 5 km, all characterized by predominance of conductive heat transfer into the U-tube. The T2Well-EOS1/TOUGH2 software suite was used within this analysis, and a preliminary assessment for a 3 km injection section of an 'Eavor-Like' U-tube benchmark was made against code developed on MATLAB and OpenGeoSys (OGS). The results reveal a good match in the injection well between all three software, and the EV environment in the CLGS 'Eavor-like' U-tube prototypes leading to the highest outlet temperatures for the 1 km and 3 km vertical depths. In addition, the outlet energy flow rate for the 5 km HSR deep scenario (5.5 MW_{th}) fell within the range for single lateral U-tube thermal outputs from the literature.

1. INTRODUCTION

This paper explores a novel use of closed-loop geothermal systems (CLGS) to recover anthropogenic heat from radioactive waste stored in a future geological disposal facility (GDF). CLGS' offer alternative solutions to conventional open-loop designs, eliminating the risk of induced seismicity and groundwater contamination by ensuring that the wellbore fluid is not in direct contact with the rock (Wang *et al*., 2020). Unlocking the potential for geothermal resources will open a plethora of opportunities, especially for projects located where conventional geothermal energy extraction is difficult to achieve. This direct heat-exchange between the two media also aims to increase geothermal energy extraction in reservoir locations where permeability is lacking (Oldenburg *et al*., 2016).

A GDF has to conform to a location with low permeable rock, where fracture networks are minimal and within a tectonically stable environment (Kochkin *et al*., 2021). Development of GDF's is slow due to the struggles to gain construction approval because of political and social opposition. Despite the controversy associated with radioactive waste disposal, a long-term solution is needed to dispose of waste from past reactor operations and to reduce the liability onto future generations.

With both CLGS' and GDF's requiring unique geological environments, this paper proposes to combine both applications to harness low-carbon heat from anthropogenic sources. This could enhance the performance of CLGS', while also improving the safety of future GDF's. The latter is important when considering rock displacement effects from disposal of high heat producing wastes (HHPW). One study predicted a displacement of 1.15 m and an estimated average temperature rise of 27 °C in EV rock 5,000 years after waste emplacement (Jackson *et al*., 2016). This coupling aims to mitigate these displacement effects by safely removing excess heat via CLGS'.

An overview of the GDF and CLGS environments is presented in Section 2. The model setup was based on a benchmark case study for a single lateral 3 km by 4 km CLGS design (Yuan *et al*., 2021), where vertical injector part was used as a preliminary assessment – see Section 3.2. The methodology for the numerical/semi-analytical is provided in Section 3.1.

2. BACKGROUND THEORY

2.1 GDF Literature Studies

A GDF is designed to host a country's radioactive waste. As the radioactivity of the waste decays with time, decay heat is released to the surrounding geological formations. HHPW – spent nuclear fuel (SNF) and highly-vitrified waste (HLW) – need adequate shielding to prevent unwanted radionuclide contamination into the groundwater (RWM, 2021, p.1). The waste is therefore encapsulated in a multi-barrier layer system, offering added protection and long-term durability to the deposition tunnel the waste is emplaced within.

The depth of such a GDF can vary depending on the volume and type of waste. A conventional mined GDF, like those under construction at Olkiluoto, Finland and Forsmark, Sweden, emplaces waste in a series of deposition tunnels and panel configurations at a depth of 0.2 - 1 km (Posiva Oy, 2012; SKB, 2011). Other systems, such as the Deep Isolation Project in the US cater to small volumes of HHPW (10 – 100’s m^3) (Chapman, 2019). This concept was demonstrated in 2019 at a test site with a depth of 1.5 km but it has been suggested that the deep borehole disposal (DBD) concept could be suitable for depths up to 6 km (Beswick *et al*., 2014).

Within this study, a vertical depth for the CLGS U-tube prototype was chosen between 1 – 5 km; 1 km to cater for the upper end of shallow mined GDF’s, 3 km to cater to the mid-deep end of DBD and 5 km for the upper end of DBD – see Section 3.3 for details. The 5 km depth is representative of deep granite basement rock (Gibb *et al*., 2008a, 2008b). To cater for large repository areas present in GDF designs, this study focuses on the heat analysis from a CLGS U-tube prototype where heat is picked up via conduction only – see Section 2.2.

2.2 CLGS Literature Studies

CLGS designs include coaxial borehole/downhole (BHE/DHE) and U-tube heat exchangers (Wang *et al*., 2021b; Zhang *et al*., 2021b). The former could involve vertical, horizontal and inclined well configurations (Van Horn *et al*., 2020; Wang *et al*., 2021b). A combination of the two can also exist; such as a single (Lyu *et al*., 2017) or multi U-tube DHE (Lund, 2003) in Klamath Falls, Oregon.

Heat transfer analyses on U-tube designs have been modelled within the literature, covering a wide range of vertical depths (2.5 – 7 km), lateral depths (0.45 – 7 km) and flow rates (1 – 97 kg/s) (Beckers *et al*., 2022). Some models have assumed no thermal resistance between casing/cement material and the wellbore and hence omit these layers (Yuan *et al*., 2021), or consider casing/cement layers in the vertical sections only (Fallah *et al*., 2021). The latter describes an ‘open-lateral’ system to maximise heat extraction from the reservoir. However, to maintain GDF safety it is better practice to adopt casing and cement throughout the whole U-tube design. Other studies suggest the use of thermally enhanced casing and/or grout material in the lateral to ensure more heat is absorbed by the working fluid (Kerme and Fung, 2020; Song *et al*., 2018; Zhang *et al*., 2021b, 2021a).

The Eavor-Loop™ technology has received recent attention within the literature to deploy a CLGS U-tube heat exchanger without the need for a hot aquifer (Winsloe *et al*., 2021). The ‘Eavor-Lite’ demonstration project in Alberta, Canada recently produced a temperature increase of 30°C (inlet 20°C and outlet 50°C) after 480 days - which was reported to back up analytical, 2D axisymmetric and 3D numerical models (van Wees, 2021; Winsloe *et al*., 2021). This U-tube heat exchanger pumps water 2.2 km down, 1.7 km across, and back up the outlet to surface by use of the thermosyphon effect, claiming to eliminate the need for additional pumping costs (Eavor Technologies Inc., 2021; Holmes *et al*., 2021; Toews and Holmes, 2021). This type of CLGS is claimed to have the potential to allow exploitation of geothermal energy anywhere, especially within low temperature, low permeability environments where purely conductive heat transfer prevails (Winsloe *et al*., 2021). As the Eavor-loop design suits the GDF environment, an ‘Eavor-like’ U-tube design is incorporated into this paper.

3. METHODOLOGY

3.1 T2Well-EOS1/TOUGH2 software setup

The T2Well-EOS1/TOUGH2 software is an integrated research code catered to multi-phase non-isothermal flow, for both reservoir and wellbore domains (Pan and Oldenburg, 2014). The reservoir (TOUGH2) is solved semi-analytically for conductive flow only to avoid large computational costs. The wellbore domain (T2Well) is discretised and a 1D single-phase momentum equation is solved numerically via the Drift Flux Model (Pan *et al*., 2011) – see Figure 1 for the key equations solved within the wellbore, interpreted from (Pan and Oldenburg, 2014):

$$\frac{\partial M^{\kappa}}{\partial t} = q^{\kappa} + F^{\kappa} \quad [1]$$

$$M^{E} = \rho_L S_L \left(U_L + \frac{u_L^2}{2} + gz\cos\theta \right) \quad [2]$$

$$F^{E} = -k\frac{\partial T}{\partial z} - \frac{1}{\sigma}\frac{\partial}{\partial z}\left[\sigma \rho_L S_L u_L \left(h_L + \frac{u_L^2}{2} + gz\cos\theta \right) \right] \quad [3]$$

$$\frac{\partial}{\partial t}(\rho_L u_L) + \frac{1}{\sigma}\frac{\partial}{\partial z}[\sigma(\rho_L u_L^2 + \gamma)] = -\frac{\partial P}{\partial z} - \frac{\Gamma f \rho_L |u_L| u_L}{2\sigma} - \rho_L g\cos\theta \quad [4]$$

Figure 1: Mass, Energy and Momentum Conservation equations solved within the wellbore (T2Well).

Equations [2] and [3] define the energy accumulation (M^E) and flux terms (F^E) for the wellbore conservation equation [1] in partial derivative form. The conservation of momentum equation [4] incorporates a drift flux velocity (u_d) which is equal to zero under single-phase flow (Pan et al., 2011, p.50). Other variables quoted are: ρ_L liquid density (kg/m^3), S_L local saturation of liquid phase, U_L internal energy of liquid phase, u_L liquid velocity of fluid (m/s), g gravitational acceleration (m/s^2), z elevation in well (m), θ inclination angle of wellbore (°), k area averaged thermal conductivity of wellbore (W/mK), σ cross section area of wellbore (m^2), h_L specific enthalpy of liquid phase (kJ/kg), γ slip between two phases, f apparent friction coefficient, Γ surface area of well side (m^2) and P pressure (Pa).

The equation of state (EOS1) applied to this software is for pure water – non-isothermal – under single-phase flow conditions in the wellbore with a temperature and pressure limitation of $T \leq 350$ ℃ and $P \leq 100\ MPa$.

T2Well was previously applied to a deep borehole heat exchanger (DBHE) (Doran et al., 2021; Renaud et al., 2021) and CLGS in (Oldenburg *et al*., 2016) where water and CO_2 circulating fluids were pumped into a single U-tube configuration 2.5 km vertically, and 1.1 km across. The semi-analytical approach taken in this paper was also applied within the study of (Oldenburg *et al*., 2016).

3.2 CLGS optimal U-tube setup against benchmark

To formulate a CLGS U-tube prototype, a benchmark case study was taken from Yuan *et al*, 2021 for a single lateral case at 3 km vertical depth, 4 km horizontal length, with pure water as the working fluid at a constant mass flow rate of $\dot{m}$ = 5.47 kg/s (Yuan *et al*., 2021). Figure 2 below provides a schematic of the CLGS U-tube approach:

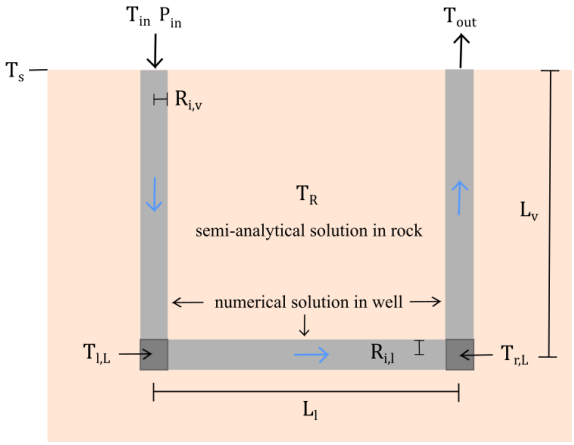

Figure 2: Schematic of CLGS U-tube, illustrating where numerical/semi-analytical modelling is applied in the wellbore/rock system. Blue arrows depict the circulation of the working fluid.

Where $T_{l,L}$, $T_{r,L}$ and T_{out} are the temperatures at the bottom of the injection well, the bottom of the production well and the outlet respectively. The other parameters are defined in Table 1 below:

Table 1: Benchmark CLGS U-tube design

Geometry vertical	***Value***
Inner radius, $R_{i,v}$(m)	0.105
Vertical depth, L_v(m)	3000
Geometry lateral	
Inner radius, $R_{i,l}$(m)	0.078
Lateral length, L_l(m)	4000
Reservoir conditions	
Surface temperature, T_s(°C)	5
Initial reservoir temperature at 3 km, $T_{i,R}$(°C)	150
Geothermal gradient, G(°C/m)	0.048
Vertical rock thermal conductivity, $k_{v,R}$(W/mK)	2.0
Rock density, ρ_R(kg/m^3)	2500
Rock specific heat capacity, $c_{P,R}$(J/kgK)	1100
Wellbore Fluid conditions	
Mass flow rate, $\dot{m}$(kg/s)	5.47
Inlet temperature, T_{in}(°C)	60
Initial wellbore pressure P_{in}(MPa)	1.3

From Table 1, all parameters have been extracted from the benchmark case study where the fluid properties were assumed to be constant. However, the T2Well-EOS1/TOUGH2 model within this paper uses non-constant water properties taken from the International Formulation Committee (1967) defined for the EOS1 in TOUGH2 (Pruess *et al*., 2012).

Prior to the 'Eavor-like' U-tube setup, the 3 km vertical injection section of the well was simulated separately in T2Well-EOS1/TOUGH2 and used as a preliminary assessment against two numerical models (see inlet section in Figure 2). The governing equations for the MATLAB code developed by (Brown *et al*., 2022, 2021) and OGS (Chen *et al*., 2019; Watanabe *et al*., 2017) also assume conductive heat flow in the reservoir and conductive/convective flow in the wellbore. The results for this 3 km injector well of MATLAB/OGS against T2Well-EOS1/TOUGH2 is highlighted in Section 4.1.

Some differences exist between the numerical solutions, particularly within the physical assumptions. MATLAB and OGS assume constant fluid properties and OGS has a slightly different initial condition for the temperature of the fluid in the pipe where it is initially set as a pre-mixed constant of 60 °C.

3.3 CLGS optimal U-tube setup GDF study

The benchmark case study assumes no casing/cement properties to neglect overall wellbore material thermal resistance. The same assumption was applied for the

GDF study; however, it should be noted that future modelling requires casing/cement layers to comply with GDF safety for a fully closed-loop system. In addition, a lower geothermal gradient of 0.026 °C/m was presumed to suit future GDF environments, to better represent low temperature environments witnessed in the UK (Busby, 2010). This geothermal gradient readjusts $T_{i,R}$ to 31, 83 and 135 °C for vertical depth prototypes of 1, 3 and 5 km respectively.

The reservoir thermophysical properties for each geology of interest are summarised in Table 2, taken from Jackson *et al*, 2016 (Jackson *et al*., 2016).

In total, seven GDF scenarios were constructed – three geology types for each vertical depth (1 and 3 km) and one HSR rock scenario at 5 km to suit granite basement rock environments (Gibb *et al.*, 2012). An initial time of 1 year was selected for a preliminary proof of concept and to allow initial comparisons between the models. To ensure viability in the ‘Eavor-like’ U-tube design within a GDF setting, the mass flow rates for each vertical case were set to 5.47, 20 and 40 kg/s for 1, 3 and 5 km respectively. All 1 km scenarios followed the CLGS parameters set from the benchmark study in Table 1 and of its associated GDF environment in Table 2. The 3 km scenarios adopt a constant mass flow rate of $\dot{m} = 20$ kg/s to follow the U-tube single lateral study adopted in (Beckers *et al.*, 2022). The 5 km scenarios were set to a lateral length of L_l = 5000 m, and $\dot{m} = 40$ kg/s to suit a mass flow rate that lies within the range of case study literature for this chosen depth (Kelly *et al.*, 2022). These preliminary scenarios assume an injection temperature similar to the surface temperature of the rock (5 °C), but future work should entail a study where injection temperature is varied. The results for the GDF study are displayed in Section 4.2.

Table 2: Reservoir thermophysical properties for GDF scenarios

HSR	***Value***
Thermal conductivity, k_H (W/mK)	3.0
Specific heat capacity, $c_{P,H}$ (J/kgK)	820
Density, ρ_H(kg/m^3)	2700
LSSR	
Thermal conductivity, k_{LS} (W/mK)	1.9
Specific heat capacity, $c_{P,LS}$ (J/kgK)	1400
Density, ρ_{LS}(kg/m^3)	2100
EV	
Thermal conductivity, k_E (W/mK)	4.8
Specific heat capacity, $c_{P,E}$ (J/kgK)	860
Density, ρ_E(kg/m^3)	2500

4. RESULTS

4.1 CLGS benchmark comparison

Figure 3 depicts a comparison between T2Well’s numerical/semi-analytical, MATLAB numerical and OGS numerical approaches to wellbore temperatures for 1 year seen at the bottom of the injection well ($T_{l,L}$):

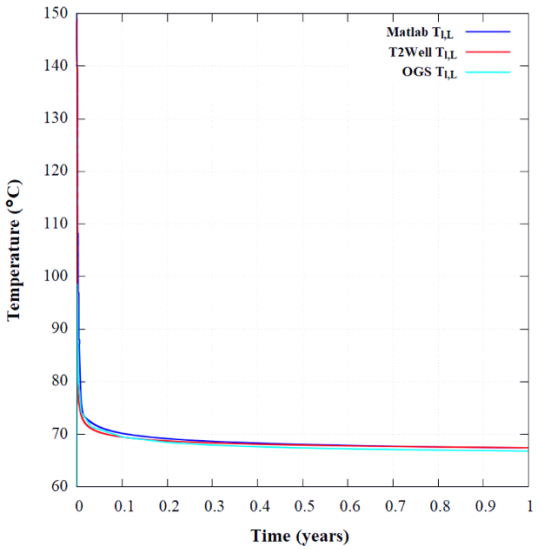

Figure 3: Comparison of T2Well numerical/semi-analytical versus MATLAB and OGS numerical approaches to key wellbore temperatures at 3 km depth (1year).

From Figure 3, all three software show a good comparison in the temperature profile down the left vertical well, with T2Well yielding $T_{l,L}$ = 67.44 °C after 1 year while MATLAB and OGS show percentage differences of 0.04 % and 0.9 % and temperature profiles of 67.41 °C and 66.8 °C respectively. These subtle differences could be due to T2Well assuming non-constant water properties, while MATLAB and OGS are constant, and this could influence the specific heat capacity, thermal conductivity and density of the working fluid as it travels down the injector.

Future work could entail a more detailed software comparison between T2Well-EOS1/TOUGH2, MATLAB and OGS. In particular, the full numerical version of the T2Well-EOS1/TOUGH software suite could then be compared against both MATLAB and OGS to accurately assess validity and any potential discrepancies between the numerical models.

This study also provides preliminary results that are suitable for short timescales of 1 year, to achieve proof of concept. Future work should also entail simulations over a longer timescale (30 years) to incorporate an accurate depiction of the long-term sustainability of the CLGS design.

4.2 CLGS GDF study

Figures 4 – 6 illustrate the CLGS ‘Eavor-like’ U-tube prototypes as illustrated in Figure 2, at vertical depths 1km, 3km and 5 km respectively after 1 year:

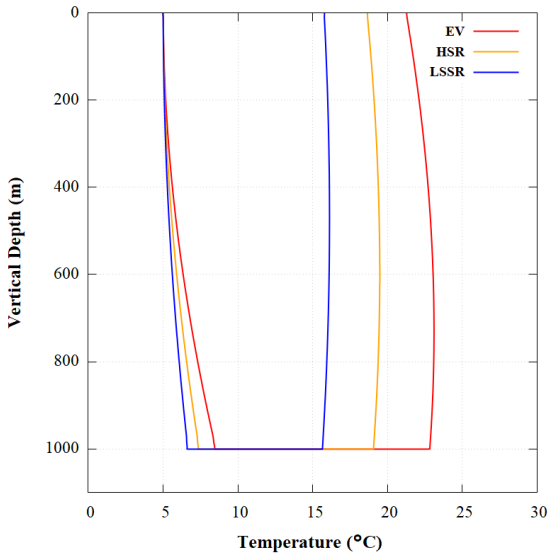

Figure 4: 1 km CLGS prototype in EV (red), HSR (yellow) and LSSR (blue) formations after 1 year at constant $\dot{m}$ = 5.47 kg/s and L_l = 4000 m.

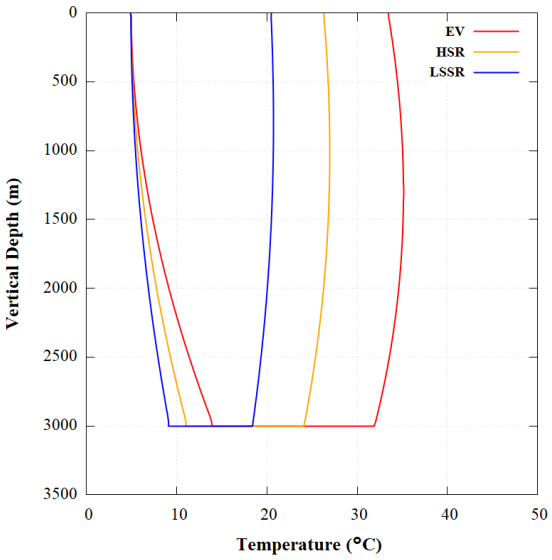

Figure 5: 3 km CLGS prototype in EV (red), HSR (yellow) and LSSR (blue) formations after 1 year at constant $\dot{m}$ = 20 kg/s and L_l = 4000 m.

Comparing all 1 km scenarios after 1 year (Figure 4), the EV geology displays the highest T_{out} = 21 °C versus 19 °C and 16 °C for HSR and LSSR respectively, due to the largest thermal diffusivity (equation [3]) correlating to a high thermal conductivity value of 4.8 W/mK within the rock. A higher thermal conductivity will increase the rate of heat transfer into/out of the CLGS U-tube prototype and hence the desired outlet temperature. The largest ΔT = 15 °C in the lateral section was also observed in the EV geology for the 1 km scenarios.

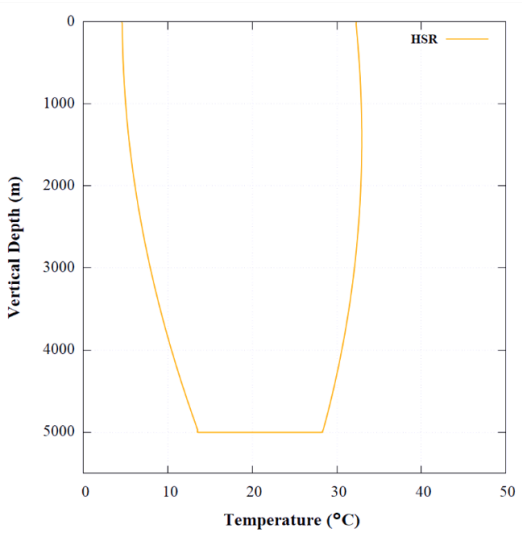

Figure 6: 5 km CLGS prototype HSR (yellow) environment after 1 year at constant $\dot{m}$ = 40 kg/s and L_l = 5000 m.

Comparing all 3 km scenarios after 1 year (Figure 5), T_{out} = 33 °C is the highest outlet temperature for the EV case versus 26 °C and 20 °C for HSR and LSSR respectively. For the HSR case, T_{out} is very similar to T_{out} = 30 °C reported within the literature for a single U-type lateral design after 1 year; with similar parameters in rock thermophysical properties, geothermal gradient and mass flow rate (Beckers *et al.*, 2022). Like the 1 km comparison, EV also yields the highest ΔT = 18 °C in the lateral section versus 13 °C and 9 °C for the HSR and LSSR lateral sections respectively. Increasing the vertical depth from 1 km to 5 km also increases T_{out} as expected from the literature (Beckers *et al.*, 2022; Lyu *et al.*, 2017). For example, $T_{l,L}$ has increased approximately by 6 °C within the HSR formation. However, it is worth noting that the constant mass flow rate is higher for the 3km and 5 km scenarios so this could also be an influencing factor to the temperature profile. However, according to (Wang *et al.*, 2021a) T_{out} will decrease following a rise in mass flow rate at a fixed vertical depth, and therefore one can assume that this increase in vertical depth is the dominating process leading to a higher T_{out} verses a higher mass flow rate.

Increasing the lateral length from 4000 m (1 km and 3 km) to 5000 m (5 km) also has an influence on heat extraction rates and the value of T_{out}. For example, the HSR geology yields a ΔT lateral increase of approximately 1.5 °C and a T_{out} rise from 26 °C to 32 °C when comparing the 3 km and 5 km scenarios respectively. Indeed, increasing the lateral length will enhance heat extraction rate and reduce overall costs, but an optimum length is desired as T_{out} could decrease and affect the overall performance of the CLGS U-tube system if the lateral length is too high (Song *et al.*, 2018; Wang *et al.*, 2021b; Winsloe *et al.*, 2021). As stated previously, other factors are also at play such as vertical depth and mass flow rate that could influence the T_{out} values. In fact, according to (Esmaeilpour *et al.*, 2021) it is favorable to increase the vertical depth

versus the lateral section for larger T_{out} values, whilst reducing completion costs (Wang *et al*., 2021b).

In general, for all prototype scenarios, the observed T_{out} values range between 16 – 33 °C. These correspond to energy rates from T2Well-EOS1 at the outlet point between 0.4 – 0.5 MW_{th} (1 km), 1.7 – 2.8 MW_{th} (3 km) and 5.5 MW_{th} (5 km). The 5 km case alone falls within the range of heat production values obtained within the literature (Beckers *et al*., 2022; Kelly *et al*., 2022). In fact, for a single lateral case, thermal power outputs from the U-tube design are reported to fall between 3 – 8 MW_{th} which is within the range obtained for the 5 km prototype scenario (Kelly *et al*., 2022). According to (Winsloe *et al*., 2021), a U-tube design could cater to heating and cooling applications if $T > 70$ °C, and anything below this is considered for ground source heat pump technology. Clearly, the outlet temperatures presented here are too low to suit U-tube heating and cooling purposes, but energy flow rates for the 5 km scenarios are well within range. However, further work is needed to quantify the geothermal gradient when an anthropogenic heat source term is incorporated into the rock. According to (Jackson *et al*., 2016, p.17), rock displacement from a future HHPW repository could see maximum temperature rises between ΔT = 30 – 50 °C within the first 100’s of years after waste deposition. This added temperature could enhance the current geothermal gradient and increase T_{out} further (Jackson *et al*., 2016, p.8). In addition, the lack of temperature could also be due to assuming a 2D discretisation in the T2Well semi-analytical approach, whereas 3D discretisation is typically seen in the literature (Oldenburg *et al*., 2016; Song *et al*., 2018; Yuan *et al*., 2021). Future work to develop the model using a 3D wellbore discretisation and semi-analytical approach is needed to further quantify these temperatures, alongside a comparison against fully numeric solutions.

3. CONCLUSIONS

In conclusion, a numerical/semi-analytical solution in the T2Well/EOS1 research code was compared against two numerical models (MATLAB and OGS) using a benchmark case study of a 3 km left vertical well, followed by a GDF study for CLGS U-tube prototype designs catered to suit a future GDF environment. In general, all three software showed a good match in temperature down the left vertical well after 1 year, with minor percentage differences of 0.04 % and 0.9 % against MATLAB and OGS respectively. The GDF study revealed that the EV environment yielded the highest outlet temperature T_{out} values due to possessing the highest thermal conductivity in the formation (4.8 W/mK vs 3.0/1.9 W/mK). Increasing the vertical depth of the CLGS U-tube prototype proved to be the dominating factor at affecting the T_{out} values versus increasing the lateral length. While $T_{out} < 70$ °C values are too low for U-tube heating/cooling applications, the energy flow rate for the 5 km scenario (5.5 MW_{th}) is within range for a typical single lateral U-tube design from the literature. Future work is needed to consider an anthropogenic heat source term to enhance the low geothermal gradient GDF environment. In addition, a 3D discretisation in the wellbore should also be compared against the 2D numerical/semi-analytical approach in T2Well as well as full numerical solutions over timescales of 30 years.

Acknowledgements (optional)

The authors would like to acknowledge additional assistance from Dr Yingqi Zhang at Lawrence Berkeley National Laboratory on modelling discussions.

Funding

This research is supported by the UK Engineering and Physical Sciences Research Council (EPSRC) [Grant number EP/R513222/1].

REFERENCES

Beckers KF, Rangel-Jurado N, Chandrasekar H, Hawkins AJ, Fulton PM, Tester JW. Techno-Economic Performance of Closed-Loop Geothermal Systems for Heat Production and Electricity Generation. Geothermics 2022;100:102318. https://doi.org/10.1016/J.GEOTHERMICS.2021.102318.

Beswick AJ, Gibb FGF, Travis KP. Deep borehole disposal of nuclear waste: engineering challenges. Proc Inst Civ Eng - Energy 2014;167:47–66. https://doi.org/10.1680/ener.13.00016.

Brown CS, Cassidy NJ, Egan SS, Griffiths D. A sensitivity analysis of a single extraction well from deep geothermal aquifers in the Cheshire Basin, UK. Q J Eng Geol Hydrogeol 2022:1–17. https://doi.org/10.1144/QJEGH2021-131.

Brown CS, Cassidy NJ, Egan SS, Griffiths D. Numerical modelling of deep coaxial borehole heat exchangers in the Cheshire Basin, UK. Comput Geosci 2021;152:104752. https://doi.org/10.1016/J.CAGEO.2021.104752.

Busby J. Geothermal Prospects in the United Kingdom. Proc. World Geotherm. Congr., Bali: 2010, p. 25–9.

Chapman N. Who Might Be Interested in a Deep Borehole Disposal Facility for Their Radioactive Waste? Energies 2019;12:1542. https://doi.org/10.3390/en12081542.

Chen C, Shao H, Naumov D, Kong Y, Tu K, Kolditz O. Numerical investigation on the performance, sustainability, and efficiency of the deep borehole heat exchanger system for building heating. Geotherm Energy 2019;7:1–26. https://doi.org/10.1186/S40517-019-0133-8/FIGURES/12.

Doran HR, Renaud T, Falcone G, Pan L, Verdin PG. Modelling an unconventional closed-loop deep borehole heat exchanger (DBHE): sensitivity analysis on the Newberry volcanic setting. Geotherm Energy 2021;9:1–24. https://doi.org/10.1186/S40517-021-00185-0/FIGURES/11.

Eavor Technologies Inc. Eavor-Loop™ Basics. Eavor Technol Inc 2021. https://eavor.com/about/eavor-loop-basics (accessed April 8, 2021).

Esmaeilpour M, Korzani G, Kohl T. Performance Analyses of Deep Closed-loop U-shaped Heat Exchanger System with a Long Horizontal Extension. 46th Work. Geotherm. Reserv. Eng., vol. 46, Stanford: 2021, p. 1–8.

Fallah A, Gu Q, Chen D, Ashok P, van Oort E, Holmes M. Globally scalable geothermal energy production through managed pressure operation control of deep closed-loop well

systems. Energy Convers Manag 2021;236:114056. https://doi.org/10.1016/j.enconman.2021.114056.

Gibb FGF, Travis KP, Hesketh KW. Deep borehole disposal of higher burn up spent nuclear fuels. Mineral Mag 2012;76:3003–17. https://doi.org/10.1180/minmag.2012.076.8.16.

Gibb FGF, Travis KP, McTaggart NA, Burley D. A model for heat flow in deep borehole disposals of high-level nuclear waste. J Geophys Res Solid Earth 2008a;113:1–18. https://doi.org/10.1029/2007JB005081.

Gibb FGF, Travis KP, McTaggart NA, Burley D, Hesketh KW. Modeling temperature distribution around very deep borehole disposals of HLW. Nucl Technol 2008b;163:62–73. https://doi.org/10.13182/NT08-A3970.

Holmes M, Toews M, Jenkins J, Sepulveda N. Multilateral Closed-Loop Geothermal Systems as a Zero-Emission Load-Following Resource. GRC Trans., Eavor Technologies Inc. and DeSolve LLC; 2021, p. 25–52.

Van Horn A, Amaya A, Higgins B, Muir J, Scherer J, Pilko R, et al. New Opportunities and Applications for Closed-Loop Geothermal Energy Systems. GRC Trans., 2020, p. 1123–43.

Jackson CP, Holton D, Myers S. Project Ankhiale: Estimating the uplift due to high-heat-generating waste in a Geological Disposal Facility . Warrington: 2016.

Kelly JJ, McDermott CI, Kelly JJ, McDermott CI. Numerical modelling of a deep closed-loop geothermal system: evaluating the Eavor-Loop. AIMS Geosci 2022 2175 2022;8:175–212. https://doi.org/10.3934/GEOSCI.2022011.

Kerme ED, Fung AS. Heat transfer simulation, analysis and performance study of single U-tube borehole heat exchanger. Renew Energy 2020;145:1430–48. https://doi.org/10.1016/J.RENENE.2019.06.004.

Kochkin B, Malkovsky V, Yudintsev S, Petrov V, Ojovan M. Problems and perspectives of borehole disposal of radioactive waste. Prog Nucl Energy 2021;139:103867. https://doi.org/10.1016/J.PNUCENE.2021.103867.

Lund JW. The use of downhole heat exchangers. Geothermics 2003;32:535–43. https://doi.org/10.1016/J.GEOTHERMICS.2003.06.002.

Lyu Z, Song X, Li G, Hu X, Shi Y, Xu Z. Numerical analysis of characteristics of a single U-tube downhole heat exchanger in the borehole for geothermal wells. Energy 2017;125:186–96. https://doi.org/10.1016/J.ENERGY.2017.02.125.

Oldenburg C, Pan L, Muir M, Oldenburg CM, Muir MP, Eastman AD, et al. Numerical Simulation of Critical Factors Controlling Heat Extraction from Geothermal Systems Using a Closed-Loop Heat Exchange Method. 41st Work. Geotherm. Reserv. Eng., Stanford: Lawrence Berkeley National Laboratory; 2016, p. 1–8.

Pan L, Oldenburg CM. T2Well—An integrated wellbore–reservoir simulator. Comput Geosci 2014;65:46–55. https://doi.org/10.1016/J.CAGEO.2013.06.005.

Pan L, Oldenburg CM, Wu Y-S, Pruess K. T2Well/ECO2N Version 1.0: Multiphase and Non-Isothermal Model for Coupled Wellbore-Reservoir Flow of Carbon Dioxide and Variable Salinity Water. Berkeley: 2011.

Posiva Oy. Olkiluoto Site Description 2011. Olkiluoto: 2012.

Pruess K, Oldenburg C, Moridis G. TOUGH2 User’s Guide, Version 2.1. Berkeley : 2012.

Renaud T, Pan L, Doran H, Falcone G, Verdin PG. Numerical Analysis of Enhanced Conductive Deep Borehole Heat Exchangers. Sustain 2021;13:1–21. https://doi.org/10.3390/SU13126918.

RWM. Inventory for geological disposal Main Report. Didcot: 2021.

SKB. Long-term safety for the final repository for spent nuclear fuel at Forsmark Main report of the SR-Site project Volume I. Stockholm: 2011.

Song X, Shi Y, Li G, Shen Z, Hu X, Lyu Z, et al. Numerical analysis of the heat production performance of a closed loop geothermal system. Renew Energy 2018;120:365–78. https://doi.org/10.1016/J.RENENE.2017.12.065.

Toews M, Holmes M. Eavor-Lite Performance Update and Extrapolation to Commercial Projects. GRC Trans., Eavor Technologies Inc.; 2021, p. 86–103.

Wang G, Song X, Shi Y, Yang R, Yulong F, Zheng R, et al. Heat extraction analysis of a novel multilateral-well coaxial closed-loop geothermal system. Renew Energy 2021a;163:974–86. https://doi.org/10.1016/J.RENENE.2020.08.121.

Wang G, Song X, Shi Y, Yulong F, Yang R, Li J. Comparison of production characteristics of various coaxial closed-loop geothermal systems. Energy Convers Manag 2020;225:113437. https://doi.org/10.1016/J.ENCONMAN.2020.113437.

Wang G, Song X, Song G, Shi Y, Yu C, Xu F, et al. Analyzes of thermal characteristics of a hydrothermal coaxial closed-loop geothermal system in a horizontal well. Int J Heat Mass Transf 2021b;180:121755. https://doi.org/10.1016/J.IJHEATMASSTRANSFER.2021.121755.

Watanabe N, Blöcher G, Cacace M, Held S, Kohl T. Theory. Geoenergy Model. III - Enhanc. Geotherm. Syst., Cham: Springer International Publishing; 2017, p. 1–110. https://doi.org/10.1007/978-3-319-46581-4.

van Wees JD. TNO - Eavor-Loop™ Audit Report - Eavor. Utrecht: 2021.

Winsloe R, Richter A, Vany J. The Emerging (and Proven) Technologies that Could Finally Make Geothermal Scalable. Proc. World Geotherm. Congr., Reykjavik: 2021, p. 1–11.

Yuan W, Chen Z, Grasby SE, Little E. Closed-loop geothermal energy recovery from deep high enthalpy systems. Renew Energy 2021;177:976–91. https://doi.org/10.1016/j.renene.2021.06.028.

Zhang W, Li W, Sørensen BR, Cui P, Man Y, Yu M, et al. Comparative analysis of heat transfer performance of coaxial pipe and U-type deep borehole heat exchangers. Geothermics 2021a;96:102220. https://doi.org/10.1016/J.GEOTHERMICS.2021.102220.

Zhang W, Wang J, Zhang F, Lu W, Cui P, Guan C, et al. Heat transfer analysis of U-type deep borehole heat exchangers of geothermal energy. Energy Build 2021b;237:110794. https://doi.org/10.1016/J.ENBUILD.2021.110794.